2018

Research on Charging Process Strategy of Airborne Compressor

Ling Yang
School of Chemical Engineering and Technology, Xi'an Jiaotong University, Xi'an, P.R. China, xuanchu1002@stu.xjtu.edu.cn

Yun Li
School of Chemical Engineering and Technology, Xi'an Jiaotong University, China, yunli@mail.xjtu.edu.cn

Pengfei Li
China Aviation Industry Qing'an Group Co., Ltd., 215757584@qq.com

Jianming Xu
China Aviation Industry Qing'an Group Co., Ltd., xa_xujm@163.com

Research on Charging Process Strategy of Airborne Compressor

Ling YANG[1], Yun LI[2]*, Peng Fei LI[3], Jian Ming XU[4]

[1]School of Chemical Engineering and Technology, Xi'an Jiaotong University,
Xi'an, P.R. China
E-mail: xuanchu1002@stu.xjtu.edu.cn

[2]School of Chemical Engineering and Technology, Xi'an Jiaotong University,
Xi'an, P.R. China
Phone:+86-029-82664554, Fax: +86-029-82664554, E-mail: yunli@mail.xjtu.edu.cn

[3]Qing'an Group Co., Ltd.,
Xi'an, P.R. China
E-mail: 215757584@qq.com

[4]Qing'an Group Co., Ltd.,
Xi'an, P.R. China
E-mail: xa_xujm@163.com

* Corresponding Author

ABSTRACT

An air tank can be inflated with compressed air at anytime if the aircraft is equipped with an airbone compressor. The different inlet altitude conditions and residual tank pressures both make it difficult to plan strategy about air tank filling. This paper studied the charging performance of the filling process in these complex working conditions, and proposed an inflating strategy of airborne compressor. A dynamic model is constructed to simulate the filling process of a multi-stage compressor with finite interstage volume. It takes 6 minutes to fill a tank with 2.0 L volume from 0.101 MPa to 35 MPa, and startup process merely lasts 6 seconds. The experiment on the compressor was developed on the ground. The results validated with simulation values and shared similar evolution regularity of the pressure. The filling process at high altitude has been simulated. When residual bottle pressure is atmospheric pressure, with the altitude increasing from 0 km to 20 km, the charging time increases from 6 minutes to more than 2 hours. Besides, the charging time is proportional to the residual pressure with a negative slope at a certain altitude. The mean torque in startup process declines with altitude rise, which proves filling at high altitude does not heavy the compressor's load, as well as the electric machine control difficulty. Based on simulation results, a feasible working area satisfying ejection demand is proposed, which can be used to determine the charging time under any filling condition. In order to inflate the tank in thirty minutes, this airborne compressor must work under 19.7 km.

1. INTRODUCTION

It is convenient for the aircraft to inflate the air tank by compressor at high altitude instead of carrying high-pressure air tank. However, the suction conditions are quite different from on the ground as well as different residual tank pressures. These make it difficult to forecast the compressor working performance and inflating ability.

The focuses of the airborne compressor filling tank system are compressing and inflating. Generally two simulation methods are used for compressor parameter calculating, namely steady-state modelling and dynamic modelling. In steady-state modelling, the suction and discharge mass flow of each stage are the same at any transient moment, and

the pressure and temperature of each stage are constant. This model can be used to research on the single stage or large compressor on valve movement, heat transfer, and so on (Tuhovcak, Hejcik, & Jicha, 2016). Since the airborne compressor is designed as a four-stage swash plate compressor, which is a very compact structure resulting in greatly fluctuating interstage pressure, so it has to face dynamic model. In the dynamic modelling, the instantaneous mass flow is no longer conserved. This situation commonly occurs to some micro-compressor with more than one cylinder illustrated as refrigerator, focusing on COP improvement, optimization and consumption etc (Castaing-Lasvignottes & Gibout, 2010). These researches are usually carried out under constant or slightly variable suction and discharge pressure. However, the total pressure ratio change of the airborne compressor increases up to 20 times at different altitudes. As a result, the research centered on working performance of this airborne compressor under complex environmental conditions has to be carried.

The compressed gas inflating process has been studied in many fields like hydrogen car, natural gas application and others (Bourgeois, Ammouri, Baraldi, & Moretto, 2018), focusing on the shortest possible filling completed time and allowable gas temperature rise (Striednig, Brandstätter, Sartory, & Klell, 2014). There are two methods of filling the tank, called slow filling process, where the air is compressed by compressor and directly dispenses to a tank, and fast filling process (FFP), where the compressed air is stored in large supply tanks and filled to the tank under high pressure difference (Khamforoush, Moosavi, & Hatami, 2014). In order to reduce filling time, all of hydrogen cars and CNG stations adopt FFP, so the researches focuses on FFP. However in the case of airborne filling system, to light the weight of the whole aircraft, slow filling process has to be used for the lack of a large heavy tank. Meanwhile, because the compressed air is stable gas otherwise hydrogen, the key object is shortest possible filling time.

In this paper, a dynamic model is developed to simulate the filling process of a four-stage swash compressor with a tank. A filling experiment on the ground was carried out to valid the model. The filling processes at different altitudes and under different residual tank pressures have been investigated. The charging performances including displacement, charging time, power and torque of startup at different altitudes are analyzed. Moreover, a feasible working area satisfying demand is proposed. These results can be useful for predicting the performance of airborne compressor at high altitude and optimum design the compressor to suit working at high altitude. Most of all, they can help the pilot choose the right charging strategy.

2. THE THERMODYNAMIC MODELING

A four-stage swash plate compressor driven by a brushless DC motor compresses air to required pressure and stores it into a tank, as shown in Figure 1. The working of the compressor consists of four different physical processes: an energy supplying process for the compressor speed generation; a mechanical process for the dynamic movement of the swash, piston and valve; a pressing process for the pressure build up in the cylinders and interstage pipelines; and a filling process for the counterbalance valves movement and the filling of the filter and the tank. The compressor filling process focuses on the last three processes.

The gas in control volume is assumed as ideal gas and supposed to be macroscopically in equilibrium state. The kinetic and potential energies of the gas are neglected. It is assumed that no leakage take place in the compressor. The governing equation, energy equation, gas state equation and piston movement equation are introduced in this section.

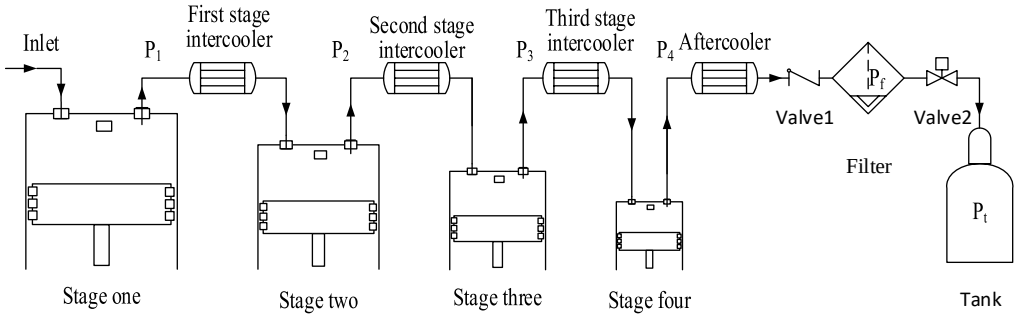

Figure 1: The schematic illustration of the filling system

2.1 Compression and Interstage Pipe Chamber

A differential formulation of conversation equation is used to model the thermodynamic process for the gas inside the cylinder and interstage pipeline. Pressure and temperature are assumed to be spatially uniform in each control volume. The changes of the working gas's potential energy and outlet kinetic energy are neglected. Based on these assumptions, energy conversation for the cylinder and interstage pipe can be written as the following equation:

$$\frac{d(mu)}{dt} = \frac{dQ}{d\theta} - \frac{dW}{d\theta} + \frac{dm_i}{d\theta} h_i + \frac{u^2}{2} \frac{dm_o}{d\theta} - h_o \frac{dm_o}{d\theta} \tag{1}$$

The compressed gas is seen as ideal gas, whose equation of state is

$$pv = R_g T \tag{2}$$

The work in cylinder is

$$\frac{dW}{d\theta} = -p \frac{dV}{d\theta} \tag{3}$$

in interstage pipe

$$dW = 0 \tag{4}$$

Ignore the outlet velocity of the air, Equation (1) can be manipulated and simplified as following: for cylinder

$$\frac{dT}{dt} = \frac{k-1}{mR_g} \frac{dQ}{dt} - \frac{(k-1)T}{V} \frac{dV}{dt} + \frac{2kT_i - (k+1)\ T}{m} \frac{dm_i}{dt} - \frac{(k-1)T}{m} \frac{dm_o}{dt} \tag{5}$$

for interstage pipe:

$$\frac{dT}{dt} = \frac{k-1}{mR_g} \frac{dQ}{dt} + \frac{2kT_i - (k+1)\ T}{m} \frac{dm_i}{dt} - \frac{(k-1)T}{m} \frac{dm_o}{dt} \tag{6}$$

2.2 Valves and Continuity Equation

The tongue spring valves are open and close mainly depending on the pressure difference between the cylinder and the suction /discharge chamber. To simulate accurate movement of thus valves is difficult for its complex geometry structure and lack of some modelling parameters. Fortunately, the filling process focuses on the pressure building up, torque and filling function, other than the valve dynamic performance. Thus, simplify the valve movement as valve opening parameter based on the pressure difference between the front and the back of the valve: 0 for the front side pressure less than the back, +0.9 for the front side pressure greater than the back while less than its 1.1 times, and +1.0 for the front side pressure greater than the back's 1.1 times.

Applying the mass conversation law for the gas as control volume:

$$\frac{dm}{d\theta} = \frac{dm_i}{d\theta} - \frac{dm_o}{d\theta} \tag{7}$$

Since it is assumed that no leak take place in the compressor, all the mass flow via the valves. The mass flow rate through each valve is modelled as incompressible instantaneous adiabatic flow through an orifice:

$$dm_j = \alpha C A_{jm} \rho_{ji} \sqrt{2(p_{ji} - p_{jo})/\rho_{ji}} \tag{8}$$

where m_j is the mass flow via the j^{th} valve, α is the valve opening parameter: 0, +0.9 and +1, C is a variable discharge coefficient which accounts for the reduced flow area resulting from the separated flows and changes with the valve lift, A_{jm} is the maximum flow area of the j^{th} valve, ρ_{ji} is the inlet gas densiy of the j^{th} valve, p_{ji} and p_{jo} are the inlet and outlet gas pressure flow through the j^{th} valve.

2.3 Piston Movement and Torque Equation

The swash plate compressor contains four cylinder. The exact expression for the instantaneous position of the piston displacement of the first stage cylinder from top dead center in terms of the crank angle may be given by:

$$x(\theta) = R_d \cdot \tan(\beta) \cdot (1 - \cos(\mathrm{wt})) \tag{9}$$

where R_d is the diameter of the cylinder distribution circle, β is the swashplate angle.

The instantaneous volume of cylinder is:

$$\mathrm{V}_c = A_c \cdot (1 + \alpha_1) \cdot x(\theta) \tag{10}$$

where α_1 is the clearance volume coefficient; A_c is the area of the cylinder.

The compressor combined rod load F_p consists of F_a, the reciprocating inertial force, F_f, the reciprocating friction force and F_g, the gas force, shown as the following

$$F_{p,j} = -\left(p_j - p_0\right) A_{p,j} + m_j R_d \omega^2 \tan\alpha \cos\theta + \frac{A_{p,j}}{16}\left(P_s + P_d\right)\left(\frac{1}{\eta} - 1\right) \tag{11}$$

where m_j is the reciprocating mass, and p_0 is the axial gas pressure.

The total load torque M_l, composed of the operating torque M_t and the friction torque M_f, is only up to the combined rod load F_p, as the following functions shown

$$M_I = F_p R_d \tan\alpha \sin\theta + f\left|F_p\right| R_d \tag{12}$$

where f is the friction coefficient.

2.4 Heat Transfer Equation

For an air compressor with double-pipe water cooling heat exchanger, the heat transfer contains three parts: gas side convection in cylinder and interstage; metal conduction and cooling water side convection. The instantaneous heat exchange is

$$\frac{dQ}{d\theta} = \frac{t - t_0}{\omega\left(\frac{1}{h_g A_g} + \frac{1}{h_l A_l} + \frac{\ln\left(d_2/d_1\right)}{2\pi\lambda l}\right)} \tag{13}$$

where t_0 is the coolant's temperature, A_g is the heat transfer area in gas side, A_l is the heat transfer area in liquid side, h_g is the heat transfer coefficient in gas side and h_l is the heat transfer coefficient in liquid side. A_g and A_l can be calculated by the structural parameters. h_g and h_l can be calculated by empirical correlation formula, for the cylinder, according to (Farzaneh-Gord, Niazmand, Deymi-Dashtebayaz, & Rahbari, 2015)

$$h = 3.26D^{-0.2} p^{0.8} T^{-0.55} v^{0.8} \tag{14}$$

where the correlation velocity is given as:

$$v = 2.28 S_p \tag{15}$$

Where S_p is the average velocity of piston, for the interstage pipe,

$$Nu_f = \frac{hd}{\lambda} = 0.023 \mathrm{Re}_f^{0.8} \mathrm{Pr}_f^{0.3} \tag{16}$$

2.5 Counterbalance Valve and Tank

The compressed air out of the fourth stage flows via two counterbalance valves before and after the filter to purge and then is filled into tank. Since the compressed air contains little impurity, all of the gas discharge the filter is assumed to fill to the tank. The mass conversation for the filter can also be given as Equation (7).

The instantaneous mass flow rate m of a certain diameter valve can be obtained from the following formula calculation:

$$dm = -\left| \frac{\sqrt{2}\mu s p_i \varphi}{\sqrt{RT_i}} \right| dt \tag{17}$$

where s is the open area of the valve; μ is the gas flow coefficient; p_i and T_i are the instantaneous pressure and temperature of gas in front of the valve; φ is the flow coefficient which depending on the pressure before and after the valve.

3. RESULTS AND DISCUSSION

3.1 Experiment and Validation of Model

A four-stage swash plate compressor driven by a brushless DC motor is designed to fulfill filling task and validate the numerical method discussed above, shown in Figure 1. The air is sucked into the compressor under atmospheric pressure, and then compressed to 35 MPa into a filter (1.3 L) and a take (2 L) after cooled to local temperature. Once the air pressure of the fourth interstage pipe and filter ups to 28 MPa and 31 MPa respectively, the two valves will turn on. If the pressure downs to 23.5 MPa and 28 MPa respectively, they will be turned off. The aeronautical coolant (volume quantity 5 L/min) divides into two streams, one passing through the aftercooler and the second-stage intercooler, the other through the third-stage intercooler and the first-stage intercooler, and then converge as one stream to cool the cylinder in the order of stage one, stage two, stage three and stage four.

Table 1: The comparison of the pressure and pressure ratio between simulating and design

Stage	Simulation Discharge Pressure/MPa	Design Discharge Pressure/MPa	Simulation Pressure Ratio	Design Pressure Ratio
Stage One	0.516	0.463	5.11	4.58
Stage Two	2.519	1.984	4.88	4.29
Stage Three	9.616	7.943	3.82	4.00
Stage Four	35.000	35.000	3.64	4.41

Table 1 shows the comparison of the pressure between simulation and design. Shown as the table 1, the pressure ratio of stage one and stage two are higher than those of design, while those of stage three and stage four are lower. Because the coolant temperature of stage one and stage two is higher and the velocity of flow is slower, the cooling

effects are worse than those of stage three and stage four. Moreover, the internal leakage also results in higher pressure of stage one and stage two. Different from the independent design of the compressor, the actual back pressure controlled by the valves and the filter has a great impact on the distribution of the pressure ratio especially on the high pressure cylinder. Thus, the simulating pressure ratios of stage three and stage four are lower than design. Compared with the simulation displacement 188 L/min at 1450 r/min, the actual displacement is 140 L/min measured by experiment. The charging time is 6 minutes, which is 1 minutes less than measured, which shows that there exists leakage in the experiment. Meanwhile, the torque ripple of the electric motor in experiment also leads to less displacement than simulation.

The pressure varies during the whole filling process is depicted in Figure 2. The actual pressure waves of AB period (from 23.5 MPa to 28 MPa), CE period (from 28 MPa to 31 MPa) and step growth of DE period (from 0.101 MPa to 31 MPa) are simplified to line for clear expression. It can be first seen that there are five turning points here. The whole filling process can be divided into three procedures. In the first procedure (before point A), the compressor starts up and compresses the air to 28 MPa, when the valve 1 turns on firstly. After the fulfillment of startup, the discharge pressure of the first two stages nearly remains constant, and that of the third stage has a slight rise with back pressure rise. During the second procedure (from point A to point D), the valve 1 is turned on intermittently by pressure difference to inflate the filter until the filter pressure is 23.5 MPa. Then valve 1 is kept open. After the pressure inside the filter increasing up to 28 MPa, the discharge pressure of the fourth compression stage increases with the filter until 31 MPa when the valve 2 is turned on firstly. In the third procedure (after point D), the valve 2 is turned on intermittently to inflate the tank till the pressure inside ups to 28 MPa. After that, the valve 2 is kept open and the pressure of the three volumes including the fourth interstage pipe, filter and tank, raise during the same time. The evolution regularity of the pressure simulated agrees with experiment.

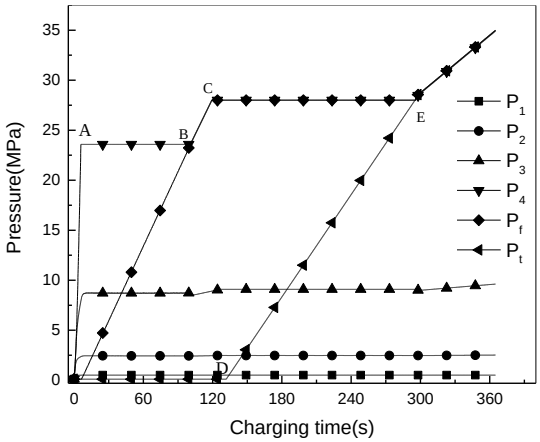

Figure 2: Variation of interstage pipe mean pressure and the pressure inside the filter and the tank vs. charging time based on the filling modelling on the ground.

3.2 Variable Altitude Filling Performance

All the filling process is developed while the aircraft flying, except that on the ground (0 km). It is assumed that the Mach number of the aircraft while flying is 0.8. There is 5% pressure loss of the air from the inlet of the air entraining pipe to the compressor's intake buffer. The air suctioned from outside during filling process in the air is compressed from stagnation state to 35 MPa through the compressor. However, when on the ground (at 0 km), due to the aircraft's motionless, the pressure and temperature of the inlet air of the compressor is equal to the atmospheric. With the rise of altitude, the atmospheric pressure reduces from 0.101 MPa to 0.005 MPa at 20 km and the atmospheric temperature reduces from 15°C to -56°C above 12 km. The charging performance at different altitudes is investigated in Figure 3.

Since the discharge pressure of the first compression stage keeps mostly unchanged after startup as mentioned above and the startup time is relatively short compared with the whole charging time, the displacement can be considered as approximately constant in the whole filling process. Figure 3(a) shows displacement of the compressor at different altitudes. It can be seen that the displacement increases from 188 L/min on the ground to 194.5 L/min at 4

km, and decreases to 144 L/min at 20 km, 26% less than that at 4 km. The main reason for the displacement on the ground less than that at 2 km is that its suction pressure, atmospheric pressure (0.101 MPa), is less than the suction pressure, stagnation pressure (0.113 MPa), at 2 km. The mass displacement from 2 km to 20 km is always descending. The displacement at 2 km less than that at 4 km is for lower density. Since the clearance volume ratio of the first compression stage is 0.1, which may decline the displacement of the compressor sharply with the first compression stage's pressure ratio rise.

Figure 3(b) gives the charging time at different altitudes. The charging time increases from 6 minutes to a little more

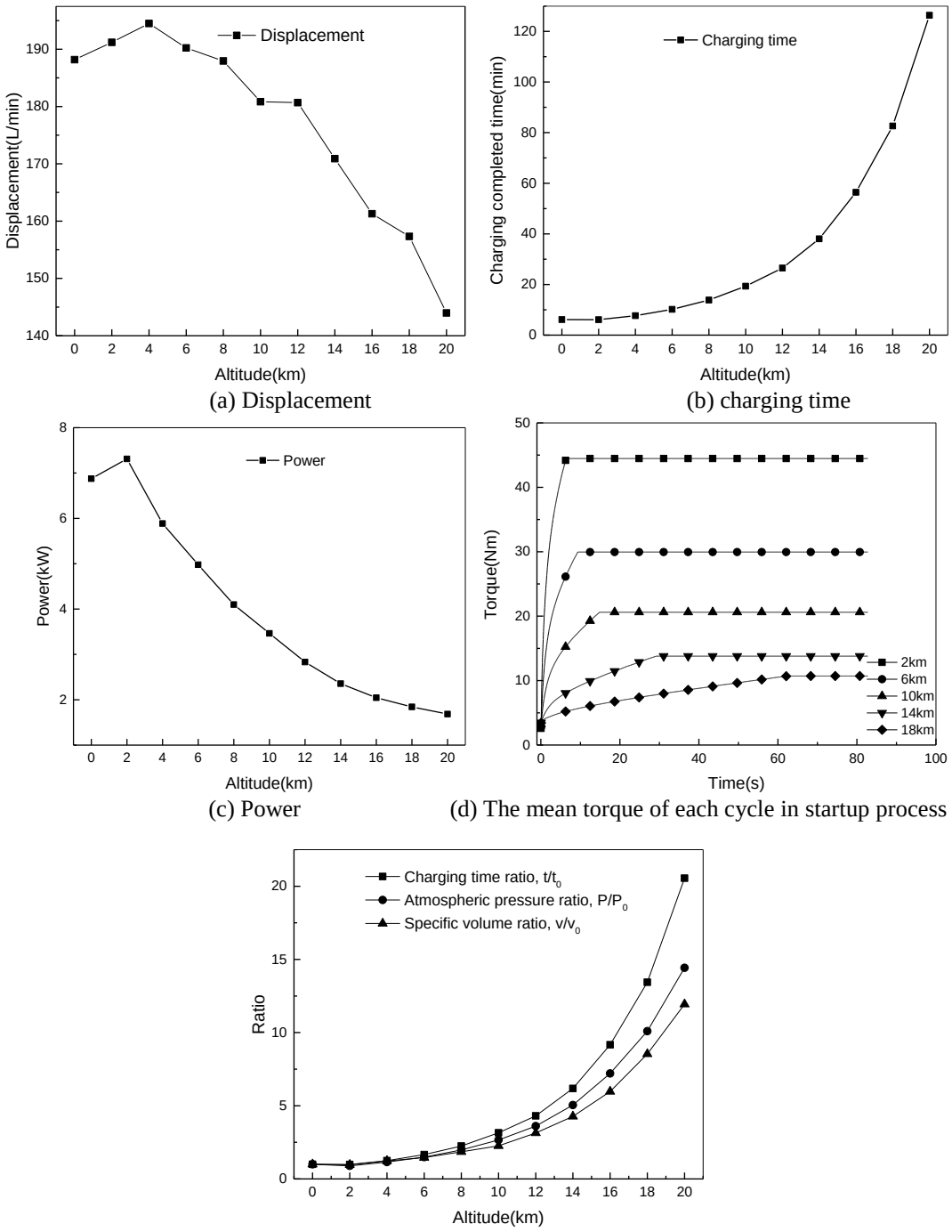

(a) Displacement (b) charging time

(c) Power (d) The mean torque of each cycle in startup process

(e)The ratio of charging time, atmospheric pressure and specific volume

Figure 3: Performance parameters and charging time under different altitudes

than 2 hours at 20 km. That is because that the air at very high altitude gets thinner and thinner, which resulting in less suction mass flow rate and less effective volume.

The electric motor's power increases with the rise of the compressor's back pressure. When the pressure inside the tank reaches to 35 MPa, the power at this moment is maximum. Figure 3(c) gives the maximum power in the whole charging process at different altitudes. The first point represents that power on the ground. The maximal motor power decreases with altitude's rise. The reason is that although the total pressure ratio of this compressor increase with altitude rise, the pressure inside the same cylinder is reducing, contributing to less torque. This rule indicates that the motor experimented on the ground is able to work at high altitude.

Figure 3(d) gives the mean torque of each work cycle change in startup process at different altitudes. The startup time extends with altitude rise especially when altitude exceeding 10 km, only 6 seconds at 2 km while up to 62 seconds at 18 km. Because the discharge pressure at the end of startup process remains 28 MPa at any altitude, resulting in the same mass of air filling all interstages of the compressor at the end of starting up. Moreover, the pressure and density of the atmospheric gas decrease with altitude rise, which makes inlet mass flow rate in each unit time reduce. The mean torque reduces form 44.5 N·m to 10.8 N·m for the discharge pressure of the first three compression stages declines with altitude rise. Moreover, the mean torque at the first three to five compression cycles increases slightly from 2.6 N·m at 2 km to 3.4 N·m at 18 km. This fluctuation compared with the load torque fluctuation is very small. In a word, working at a high altitude does not heavy the compressor's load, as well as the electric machine control difficulty.

The different altitude conditions mainly contain two variables, atmospheric pressure and temperature. Both of the two variables can be reflected by specific volume. In order to compare the charging time between in the air and on the ground intuitively, take the value of the charging time, atmospheric pressure and specific volume of air on the ground as unit value. The values at other altitudes can be calculated as t/t_0, v/v_0, and P_0/P, where t is charging time at local altitude, v and p are stagnation specific volume and stagnation pressure at that altitude and under 0.8 Mach of aircraft velocity. As shown in Figure 3(e), all of the three ratios raise with altitude rise. Compared with the specific volume ratio, the atmospheric pressure ratio is closer to charging time ratio, which indicates the actual factor of filling the tank at different altitudes is the pressure. Below 10 km, the t/t_0 and P_0/P are nearly the same. Above 10 km, the clearance volume makes the t/t_0 and P_0/P gap wider and wider. Based on this result, for the same compressor, no matter what volume the air tank is, the charging time at any altitude below 10 km can be quickly assessed by the plus of the pressure ratio and changing time measured on the ground even if there isn't experiment in the air. Above 10 km, the clearance volume shows a greater influence on displacement and charging time, so the pressure ratio can not be used to forecast charging time.

3.3 Variable Residual Tank Pressure Filling Performance

Considering the actual filling process of the aircraft, there are two cases filling situations, filling with no compressed air in both the filter and air tank and filling when some compressed gas in the air tank used. The first case has been studied in variable altitude filling process. Assuming that the filter pressure is 28 MPa at startup, the second filling case under different residual air tank pressure is calculated. Since the startup process under any residual tank pressure is to compress the air from stagnation pressure to the filter pressure, which remains 28 MPa before the next filling, the startup process is the same with the process shown in Figure 3(d). Otherwise, all the compressor's working parameters under different residual tank pressures, such displacement, power, and torque are the same with those at the same altitude as mentioned.

Figure 4 gives the 3-D curve of the altitude, residual tank pressure and charging time. All the charging times are obtained by assuming that the filter pressure is 28 MPa at startup and the velocity of the aircraft assumed before. It can be seen that the charging time decreases linearly with residual tank pressure rise at the same altitude. Because the displacement is stable, the charging time is proportionate to the gas supply of the tank, which is only up to residual tank pressure at the same altitude. Under the same residual tank pressure, the rising rate of the charging time increases with the altitude for the drop of displacement.

3.4 Feasible Working Area and Charging Process Strategy

Figure 5 gives a feasible working area, which can help the pilot chose a suitable charging strategy. The isotime curve of charging time becomes denser and denser as the altitude increases. At the same altitude, by filling the tank under a high residual tank pressure can reduce the charging time. Besides, under the same residual tank pressure,

filling at low altitude can also achieve the same goal. For example, if 30 minutes is required as the maximum charging time, the pilot can choose under any residual tank pressure to filling below 14.6 km. In order to fill the tank at a higher altitude, the residual tank pressure should be higher. The highest allowable altitude is 19.7 km. Over this altitude, the compressor could not fill the tank within 30 minutes.

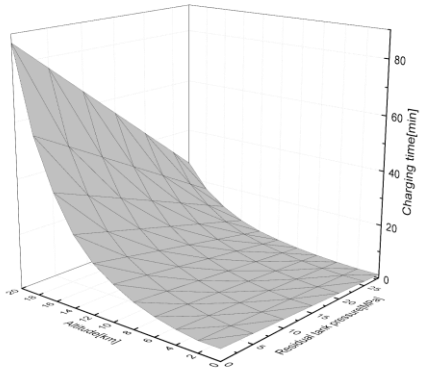

Figure 4: The 3D curve of the altitude, residual tank pressure and charging time

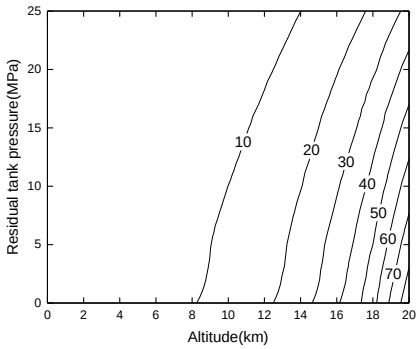

Figure 5: Feasible working area

4. CONCLUSIONS

A dynamic model of a filling system containing a multi-stage compressor with counter, valves, a filter and a tank is established to simulate the filling processes at different altitudes and under different residual tank pressures. An experiment on the ground is carried out to confirm with the model. From the results of the investigation, the following conclusions are obtained:

- The simulation pressure variations in the filling process are consistent with that of the experiment on the ground. The displacement of the compressor nearly keeps stable, and the charging time is 6 min, 1 min less than the experiment because of leakage.
- The displacement declines with the altitude rise. At 20 km, the displacement is 26% less than that at 4 km. The charging time is expanded with altitude growth, and increases up to nearly 2 hours at 20 km, more than 20 times of that on the ground. Below 10 km, charging time ratio is almost agree with atmospheric pressure ratio. At a higher altitude, the clearance volume shows a greater influence on displacement and charging time.
- The input power decreases with the altitude rise, which indicates that the motor experimented on the ground is able to work at high altitude. Besides, the mean torque of the compressor decreases with the rise of the altitude. Meanwhile, the startup time increases from 6 seconds at 2 km to 62 seconds at 18 km. So filling at high altitude does not increase the compressor's load as well as the electric machine control difficulty.
- Based on the figure of feasible working area, the required charging time restricts the highest altitude of filling. The charging time can be reduced by flying to a lower altitude or filling under a higher residual tank pressure. The highest altitude for filling in 30 minutes is 19.7 km.

REFERENCES

Bourgeois, T., Ammouri, F., Baraldi, D., & Moretto, P. (2018). The temperature evolution in compressed gas filling processes: A review. *International Journal of Hydrogen Energy, 43*(4), 2268-2292. doi:10.1016/j.ijhydene.2017.11.068

Castaing-Lasvignottes, J., & Gibout, S. (2010). Dynamic simulation of reciprocating refrigeration compressors and experimental validation. *International Journal of Refrigeration, 33*(2), 381-389. doi:10.1016/j.ijrefrig.2009.10.007

Farzaneh-Gord, M., Niazmand, A., Deymi-Dashtebayaz, M., & Rahbari, H. R. (2015). Thermodynamic analysis of natural gas reciprocating compressors based on real and ideal gas models. *International Journal of Refrigeration*, *56*, 186-197. doi:10.1016/j.ijrefrig.2014.11.008

Khamforoush, M., Moosavi, R., & Hatami, T. (2014). Compressed natural gas behavior in a natural gas vehicle fuel tank during fast filling process: Mathematical modeling, thermodynamic analysis, and optimization. *Journal of Natural Gas Science and Engineering*, *20*, 121-131. doi:10.1016/j.jngse.2014.06.009

Striednig, M., Brandstätter, S., Sartory, M., & Klell, M. (2014). Thermodynamic real gas analysis of a tank filling process. *International Journal of Hydrogen Energy*, *39*(16), 8495-8509. doi:https://doi.org/10.1016/j.ijhydene.2014.03.028

Tuhovcak, J., Hejcik, J., & Jicha, M. (2016). Comparison of heat transfer models for reciprocating compressor. *Applied Thermal Engineering*, *103*, 607-615. doi:10.1016/j.applthermaleng.2016.04.120